Fuel 325 (2022) 124920

Contents lists available at ScienceDirect

Fuel

journal homepage: www.elsevier.com/locate/fuel

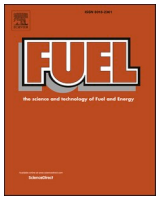

Full Length Article

Methane storage scale-up using hydrates & metal organic framework HKUST-1 in a packed column

Shurraya Denning, Ahmad A.A. Majid, James M. Crawford, Jonathan D. Wells, Moises A. Carreon *, Carolyn A. Koh *

Chemical and Biological Engineering Department, Colorado School of Mines, Golden, CO 80401, United States

ARTICLE INFO

Keywords:
Metal organic framework
HKUST-1
Gas hydrates
Hydrate growth promoter
Gas storage
Packed column

ABSTRACT

As the demand for energy rises, so does the need for storing natural gas. Gas hydrates offer a unique opportunity as they consist of water and gas, and can hold up to 160 m^3 of methane (at STP) in 1 m^3 of hydrate. Combining gas hydrates with the metal organic framework HKUST-1 produced synergistic improvements for methane storage. This study scaled the system from 0.5 cm^3 in a differential scanning calorimeter to 60 cm^3 in a packed column with a volume, with highly reproducible results, and provided insight into how HKUST-1 affects the kinetics of methane hydrate formation. For the system with HKUST-1 concentration of only 1.0 wt% and at operating conditions tested, the hydrate nucleation induction time reduced on average by 86.2 ± 5.4%, the amount hydrates formed increased by 47.7%, and the rate of hydrate growth increased on average by 7.0 times. Additionally, the system with HKUST-1 operated optimally above the freezing point of ice, unlike a system without HKUST-1, and thus requires less energy to form hydrates. This scalability of performance and positive kinetic effect shows that the combination of HKUST-1 and gas hydrates produce a promising candidate for a commercial method to store and transport natural gas.

1. Introduction

The rapid population growth worldwide results in an ever increasing demand for energy.[1] A heavily consumed energy source is natural gas due to its high heating value, abundancy worldwide, and since it burns cleaner than most fossil fuels.[2] Currently, the storage and transportation of natural gas are two areas in which more efficient methods could be applied. Common methods for storing and transporting natural gas include liquefaction (energy intensive to cool to 111 K) and compression (highly explosive). [3] An alternative, more environmentally friendly method is the utilization of gas hydrates.[4,5].

Gas hydrates are an ice-like structure that encapsulates guest molecules, such as methane, and typically form under high pressure and low temperature conditions.[6] Methane hydrates can store approximately 160 cm^3 of methane (at STP) in 1 cm^3 of hydrate, making hydrates desirable for storage purposes.[6] A kinetic anomaly, known as 'self-preservation', allows storage of methane hydrates at ambient pressure and temperature below the melting point of ice, which reduces safety risks.[3].

Two aspects of methane hydrate formation that are barriers to commercialization of this storage and transportation approach are low water-to-hydrate conversion and long hydrate nucleation induction times.[7,8] Many approaches are being studied to combat these issues, such as chemical additives (e.g. THF[9,10], SDS[11], leucine amino acid [12], boric acid[13]), apparatus design (e.g. stirred tank,[14] bubble column[15], fixed bed column[16]), and porous materials (e.g. silica gel [17,18], zeolites[19–23], activated carbon[24,25]).

Chemical additives provide a range of effects, ranging from thermodynamic (THF shifts the formation conditions to milder temperature and pressure)[9] to kinetic (SDS speeds up the growth rate and overall conversion)[11]. Apparatus designs often aim to increase the gas-to-water contact area by agitation (mechanical stirring of a tank[26,27] or by dispersing the water (void spaces in a fixed bed column[16]), as hydrate formation usually takes place at that interface and forms a barrier between the water and gas phases.[28] Porous materials also increase the gas-to-water contact area due to their large surface areas (high surface area activated carbon)[29], and the pores can provide favorable nucleation sites (micropores in RHO zeolite)[19]. The types of materials range from macroporous (silica gel)[18], mesoporous (model carbons)[30], to microporous (5A type zeolite)[23]. The chemistry of

* Corresponding authors.
E-mail addresses: mcarreon@mines.edu (M.A. Carreon), ckoh@mines.edu (C.A. Koh).

https://doi.org/10.1016/j.fuel.2022.124920
Received 28 March 2022; Received in revised form 6 June 2022; Accepted 14 June 2022
Available online 21 June 2022

the porous materials also plays a role in its effect on conversion and nucleation, such as hydrophobicity[31,32] and thermal conductivity [33].

Multiple studies discovered synergistic effects when combining these different approaches. One study put cetyl trimethyl ammonium bromide (CTAB) in with copper nanoparticles, which worked synergistically to reduce the induction time and increased the growth rate.[34] Another study observed that combining THF and hollow silica resulted in hydrates forming at almost ambient temperature (293.2 K) and moderate pressure, and adding SDS reduced the induction time by half.[35].

An understudied group of porous materials that show high potential as a hydrate formation promoter are metal–organic frameworks (MOFs). An extensive list of studies on MOFs are the following: ZIF-8, [18,31,32,36] ZIF-67,[36] Y-shp-MOF-5[37], Cr-soc-MOF-1,[37] MIL-53,[38] MIL-53(Al),[18] MIL-101,[39] MIL-100(Fe),[31] and HKUST-1. [18,40] MOFs typically have large surface area, tunable porosity, and are chemically diverse.[41] Notably, MOFs themselves are studied for gas storage[42] with particular interest in methane storage due to certain MOFs exhibiting high affinity for methane adsorption.[43] The advantage of combining MOFs with hydrates is that hydrates can increase the overall amount of methane stored in a MOF, such as found in a study on ZIF-8[31], and that after hydrate formation with the porous materials, the self-preservation phenomena common to hydrates could allow the stability conditions of ambient pressures and low temperatures,[44] whereas methane adsorption in MOFs alone often takes high pressure to maintain the storage.

A previous study from our group investigated the effects of varying the saturation of a MOF called HKUST-1, which contains copper nodes linked with organic ligands, on methane hydrate water-to-hydrate conversion.[40] In a high pressure differential scanning calorimeter (HP-DSC), addition of HKUST-1 to the methane/water system increased the water-to-hydrate conversion from 5.9% to as high as 87.2%.[40] Although this study is significantly impactful on furthering the understanding of the influence of metal organic frameworks on methane hydrate growth, the results from the HP-DSC were on a microscale and only provided a brief investigation into the kinetic effects of HKUST-1 on methane hydrates. On this previous work, we have performed an investigation at micro-level on understanding the formation kinetics of methane hydrates in the presence of HKUST-1 [40]. The results of this investigation have shown a positive outcome of HKUST-1 in the formation kinetics of methane hydrates. Motivated by these results, in this current work, we have investigated the scalability of HKUST-1 in improving the hydrate formation kinetics. The impact of HKUST-1 on the kinetics of methane hydrate growth needs a more in-depth study, and the results must be able to translate to a larger, macroscale system for future commercialization.[45].

Several studies have been performed to investigate the challenges of hydrate formation in large scale setup. In an investigation conducted by Susilo et al, sH hydrates were formed from ice particles that acted as particle seed to promote the nucleation of hydrates. In the work, high conversion of hydrate was achieved. However, the authors reported that hydrate growth rate was reduced due to mass transfer limitation created by the formation of hydrate film. [46]. One promising macroscale system is a packed column.[47] A study comparing the performance of a stirred vessel and a column packed with silica sand found that the column promoted faster hydrate growth and higher water-to-hydrate conversion as compared to the stirred tank.[16] This conspired due to the better water dispersion on the packing resulting in a higher gas-to-water contact area relative to the agitated system.[16] The conclusions from this study indicates that combining a packed column with microporous materials may exhibit excellent promotion results. In the case of microporous materials such as MOFs, the cost of the material makes packing the entire column with it economically unfavorable. Instead, the more economically advantageous route is to disperse or coat a cheap packing material with the MOF.

2. Materials & methods

2.1. Materials

HKUST-1 was purchased from ACS Materials and synthesized via a hydrothermal method. The packing material used in the column was Chenille fabric, purchased from Joann Stores, LLC. UHP Methane from Matheson was used in this work. UHP Methane was chosen in this work to minimize any metastable condition during hydrate formation that may be present when additional gas composition is added into the system.

2.2. Characterization methods for HKUST-1

The HKUST-1 material was characterized via powder X-ray diffraction, which was obtained using a Siemens Kristalloflex 810 diffractometer that utilized Cu Kαl radiation at a wavelength of 1.54059 Å, and operated at a current of 25 mA and a voltage of 30 kV. Field emission scanning electron microscopy, JOEL JSM-7000F, was used to observe the morphology of HKUST-1 before and after subjecting the material to hydrate formation and dissociation in the packed column. The surface area and porosity of HKUST-1 were determined using a nitrogen isotherm at 77 K and a methane isotherm at 20 °C after degassing the sample at 300 °C for 10 h, measured via an ASAP 2020 porosimeter (Micromeritics, Norcross, GA, USA).

2.3. Packed column apparatus

The schematic of the packed column apparatus used in this work is given in Fig. 1.[47] A stainless steel tube with an internal diameter of 1.27 cm, length of 45.72 cm, and a total volume of 60 cm^3 was used as the column in which hydrate formation would take place. The HKUST-1 was dispersed onto the packing material, chenille fabrication, by first mixing a specified amount of dry HKUST-1 into deionized water. The water and HKUST-1 was mixed until the HKUST-1 was completely dissolved, and then the chenille fabric was put into the solution. The fabric was wrung out and weighed to determine the amount of water present in the system. The packing was inserted into the column and then connected to an ISCO pumps and a back pressure regulator. ISCO pump was used to control the flow of the gas into the column while back pressure regulator was used to maintain constant experimental pressure. A cooling jacket was put around the column to control the temperature. Following this step, the system was flushed with methane gas to remove residual air. The system was pressured to the experimental pressure of 1160 psig, and then held at 20 °C for 1 h to ensure no leaks occurred. Next, the system was ramped down to our experimental temperature of −10 °C at a rate of ~0.5 °C/min and held for 24 h. The temperature and pressure changes in the system were measured and used to obtain the amount of gas consumed by the system and the time in which hydrate formation took place.

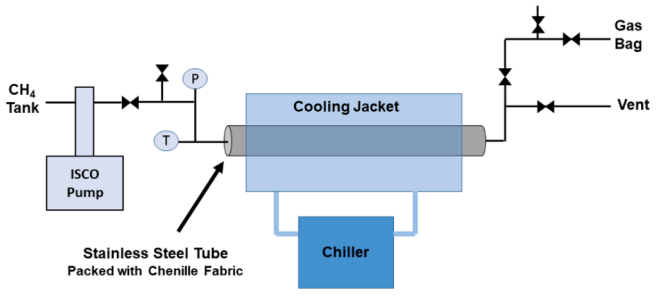

Fig. 1. Schematic of the packed column (Modified from[45]).

2.4. Calculations for volume of hydrates formed in packed column

The volume of hydrates formed in the packed column was determined by tracing the change in the moles of gas throughout the experiment. In this experimental setup, this is done by monitoring the change in the volume of the high pressure ISCO pump. In hydrate formation, the gas molecules will be consumed and trapped inside water cages. As such, there will be a decrease in the pressure of the system due to hydrate formation. Since the experiments were conducted at constant pressure, the volume of the ISCO pump will decrease to maintain the pressure of the system.

The moles of methane consumed for hydrate formation was calculated using Eq. (1). In this equation, $n_{g,t1}$ is the moles of methane at the end of experiment (once there was no further hydrate formation), and $n_{g,t0}$ is the moles of methane at the beginning of the experiment. The moles of methane in the system were calculated using SRK equation of state using the experimental pressure (P), temperature (T), and volume of the ISCO pump (V).

$$\Delta n_g = n_{g,t_1} - n_{g,t_0} = \left(\frac{PV}{ZRT}\right)_{t_1} - \left(\frac{PV}{ZRT}\right)_{t_0} \quad (1)$$

Finally, the volume of hydrate formed in the system (V_{hyd}) was calculated using Eq. (2), whereby ρ_{hyd} is the molar density of methane hydrates at the experimental conditions[6].

$$V_{hyd} = \frac{\Delta n_g}{\rho_{hyd}} \quad (2)$$

3. Results

In our study, we investigated the synergistic effects of a macro scale packed column apparatus (schematic in Fig. 1) with microporous HKUST-1 dispersed on Chenille fabric packing (shown in SEM images in Fig. 2) on methane hydrate growth. The HKUST-1 was dispersed on the Chenille fabric by first mixing HKUST-1 at a specified wt.% in water, then submerging the Chenille fabric into the solution followed by removing the excess HKUST-1/water solution via compression until Chenille fabric reached a saturated state. Detailed experimental methods are given in the Supporting Information.

3.1. Reduction in induction time & nucleation temperature

The addition of HKUST-1 to the packed column greatly decreased the hydrate nucleation induction time, as evident from the significant gas consumption observed in the pack column as the temperature was lowered at a constant pressure (see Fig. S1). Table 1 contains the hydrate nucleation induction time results from the experiments for a system without HKUST-1 and for systems with 0.5 wt%, and 1.0 wt% of HKUST-1 at operating pressures of 4 MPa and 8 MPa corresponding to different subcooling temperatures. Table 1 reports the average nucleation time and standard deviation across repeat tests. In this work, due to the size of our data set, average nucleation time and standard deviation was used to assess data reproducibility. Additionally, t-test statistical analysis was also conducted and the results are presented in Table 1. As it can be seen from the p-value, there is evidence on the effect of HKUST-1 on hydrate nucleation time.

Table 1
The hydrate nucleation induction time in the packed column for tests completed at different pressure conditions and with no HKUST-1 compared to 0.5 wt%, and 1.0 wt% of HKUST-1.

Pressure (MPa	Subcooling Temperature (°C)	Hydrate Nucleation Induction Time (minutes)			p-test
		No HKUST-1	0.5 wt% HKUST-1	1.0 wt% HKUST-1	
8 MPa	10 °C	229.1 ± 27.1 min	17.3 ± 15.5 min	17.5 ± 4.3 min	0.003
	21 °C	88.0 ± 1.8 min	15.4 ± 0.9 min	17.1 ± 1.8 min	0.012
4 MPa	7 °C	70.1 ± 3.3 min	9.8 ± 5.0 min	11.9 ± 1.2 min	0.025
	18 °C	94.9 ± 22.8 min	12.9 ± 6.2 min	10.5 ± 0.2 min	0.042

In this work, the hydrate nucleation induction time is defined as the difference between when the packed column at a constant pressure begins the cooling process from 20.4 °C and the onset of rapid gas consumption caused by hydrate formation. For the tests at 8 MPa and a subcooling temperature of 21 °C, the introduction of HKUST-1 to the system reduced the hydrate nucleation induction time by 82.3 ± 0.6% and 80.6 ± 2.0% for HKUST-1 concentrations of 0.5 wt% and 1.0 wt%, respectively. If the nucleation time is measured at when the experiment starts the cooling process (i.e. before the system reaches the target holding temperature), then in the HP-DSC the hydrate nucleation induction time was reduced by 83.8 ± 4.0%.[40] The close agreement between the packed column and HP-DSC results indicates that the methane hydrate formation promotion capabilities of HKUST-1 scales with system size.

The addition of HKUST-1 to the system also affected the hydrate nucleation temperature, as shown in Table 2. For the experiments at 8 MPa and a subcooling temperature of 21 °C, a system void of HKUST-1 did not form hydrates until reaching the holding temperature of −10 °C. In contrast, adding HKUST-1 resulted in a higher nucleation temperature of −0.5 ± 0.5 °C and 0.5 ± 0.5 °C for 0.5 wt% and 1.0 wt%. The higher nucleation temperature is directly related to the reduced hydrate nucleation induction time, as the nucleation occurs before the system (packed column and HP-DSC) reaches the target temperature, thus forming at a temperature higher than the target temperature.

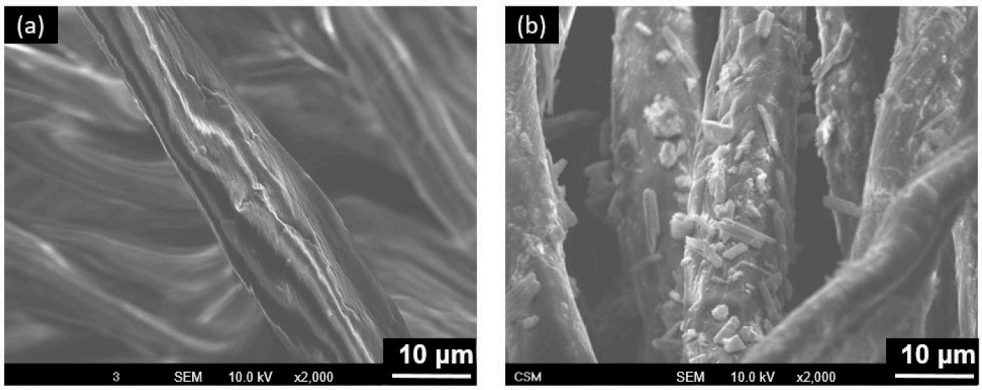

Fig. 2. SEM images of (a) Chenille fabric packing (b) HKUST-1 dispersed onto Chenille fabric.

Table 2
The hydrate nucleation temperature in the packed column for tests completed at different pressure conditions and with no HKUST-1 compared to 0.5 wt%, and 1.0 wt% of HKUST-1.

Pressure (MPa)	Subcooling Temperature (°C)	Hydrate Nucleation Temperature (°C)		
		No HKUST-1	0.5 wt% HKUST-1	1.0 wt% HKUST-1
8 MPa	10 °C	1 ± 0.5 °C	2 ± 0.5 °C	2 ± 0.5 °C
	21 °C	−10 ± 0.5 °C	−0.5 ± 0.5 °C	0.5 ± 0.5 °C
4 MPa	7 °C	1 ± 0.5 °C	1 ± 0.5 °C	1 ± 0.5 °C
	18 °C	−10 ± 0.5 °C	−2 ± 0.5 °C	−1 ± 0.5 °C

The influence of HKUST-1 on the hydrate nucleation time and temperature stems primarily from the porous crystal's thermally conductive framework and moderate wettability. The copper nodes in the structure of HKUST-1 lend to heat transferring quickly throughout the structure.[48] By dissipating the heat produced by hydrate nucleation (hydrate nucleation is exothermic process), the HKUST-1 induces a favorable environment for fast propagation of hydrate formation. As for wettability, water molecules preferentially adsorb to the copper atoms in the structure of HKUST-1 and can quickly exchange water across its structure, thus positioning water molecules in the ideal local for heat transfer as hydrate forms while also uniformly dispersing water on its surface to maximize the water-to-gas contact area.[49] Additionally, the wetted grain boundaries in HKUST-1 may act as nucleation sites, a hypothesis supported by a study in the literature that observed methane hydrate growth on microporous RHO zeolite.[19].

The wettability does come with disadvantages, as the interaction between a hydrophilic particle and the neighboring water molecules can restrict the water activity of those molecules due to the water adsorption.[31,50] A reduction in the water activity coefficient causes an impedance of the water molecules orientating themselves correctly to form the hydrogen bonds needed for the hydrate cages.[6] The HKUST-1 used in this study adsorbs approximately 13.8 mmol/g of water, as determined by the water isotherm conducted at 298 K and 1 atm given in Fig. S2, which is less than reported in the literature for this material (~22 mmol/g).[51] The noteworthy difference may stem from the surface area of commercial HKUST-1 being less than half of the surface area of the cited HKUST-1 (428 m^2/g versus 1140 m^2/g, respectively).[51] A study on the effect of hydrophobicity on methane hydrate formation using two metal organic frameworks, ZIF-8 and MIL-100(Fe), found that the hydrophobicity of ZIF-8 prevented water from clogging the crystal's pores and promoted higher methane adsorption, leading to higher water-to-hydrate conversion compared to the hydrophilic MIL-100(Fe).[31] Although HKUST-1 is not as hydrophilic as MIL-100(Fe), (13.8 mmol/g versus 31.1 mmol/g, respectively), the adsorption of water may partially fill the pores of HKUST-1, leaving less water available for hydrate formation.[31].

Methane, when adsorb on the external surface and in the pores, can promote nucleation as it can be consumed during hydrate formation, as found by studies that investigated how methane layers or bubbles at the surface of a material promote nucleation.[52,53] Therefore, the significant methane uptake of HKUST-1 contributes to its success in promoting hydrate nucleation. In this study, the commercial HKUST-1 adsorbed 0.67 mmol/g of methane at 298 K and 1 atm (isotherm shown in Fig. S3) relative to a surface area of 428 m^2/g. In the literature, one study measured methane adsorption of 1.55 mmol/g at 298 K and 1 atm relative to a surface area of 2176 m^2/g.[54] The study also measured the amount of methane adsorbed at high pressure, thus, if the results from the study are scaled appropriately, then the commercial HKUST-1 in this work should adsorb approximately 5.9 mmol/g methane at 4 MPa and 6.7 mmol/g methane at 8 MPa.[54].

The water adsorption on HKUST-1 competes with methane adsorption, as both preferentially adsorb to the copper nodes in HKUST-1.[49] Since water and methane adsorb to the same location in HKUST-1, methane may displace the water molecules and push water towards the external surface, a phenomenon observed with methane hydrate formation in the presence of microporous RHO zeolite.[19] A study on carbon dioxide, nitrogen, and hydrogen hydrate growth in the presence of HKUST-1 further supports this hypothesis, as the authors found that carbon dioxide displaced the water to promote hydrate growth, whereas neither nitrogen nor hydrogen displaced the water molecules and thus did not form hydrates.[55].

3.2. *Effects of HKUST-1 on hydrate growth rate*

The concentration of HKUST-1 in the packed column significantly impacted the amount of hydrate formed and the rate at which hydrate formation occurs. The same properties of HKUST-1 that influenced the reduction of hydrate nucleation time also play an important role here: large surface area (increases gas-to-water contact area), moderate wettability (uniformly dispersed water), fast water exchange (keeps water evenly dispersed as it supplies hydrate growth), and high methane uptake (feeds hydrate growth). As shown in Fig. 3, increasing concentration of HKUST-1 in the system up to 1.0 wt% resulted in an increase in the overall amount of hydrate formed.

It is worth to note that the Chenille fabric itself increases the gas-to-water contact area, thus providing a certain amount of hydrate growth promotion on its own, and explains why the amount of hydrate formed is higher than would be expected for a system with bulk water.[40] The addition of HKUST-1 to the packed column greatly impacted the methane hydrate growth rate. As shown in Fig. 4, as the concentration of HKUST-1 in the system increased from 0 wt% to 0.5 wt% and then 1.0 wt %, so did the growth rate. This increase stems from the thermal conductivity of HKUST-1, as it facilitated the local heat from hydrate formation to dissipate, providing a more favorable environment for continued hydrate growth. As expected, the growth rate for the high pressure experiments (8 MPa) on average was 2.4 times greater than that for the low pressure experiments (4 MPa). The higher pressure results in a higher driving force, thus it increases the mass transfer of gas to the liquid phase for hydrate formation. The experiments performed at a higher temperature with their respective pressures also showed faster growth, since at the lower temperatures ice formation competes with hydrate formation.

Interestingly, the addition of 2.0 wt% and 2.5 wt% HKUST-1 did not follow the same increasing trend. At 2.0 wt% and 2.5 wt% HKUST-1, the hydrate growth rate drastically reduced to an order of magnitude less than that of a system without any HKUST-1. This behavior aligns with the observations from our previous work studying HKUST-1 in the HP-DSC: high concentration of HKUST-1 resulted in inhibited water-to-hydrate conversion, whereas at lower concentrations HKUST-1 promoted growth.[40] Other studies on the effects of materials on hydrate growth, such as silica nanoparticles,[56] also found that as the concentration of the material increased relative to water, than hydrate growth inhibition occurred. In the case of HKUST-1, the primary cause of the hydrate promotion capabilities dependence on concentration stems from HKUST-1's rapid water uptake capacity, since the pores will uptake water and leave less free water available for hydrate formation. The pores of HKUST-1 are too small for hydrates to form within, hence, the trapped water will preferentially form ice or remain as a liquid instead of forming hydrates. When the amount of HKUST-1 in the system reaches a certain amount, as seen with the 2.0 wt% and 2.5 wt% results, the HKUST-1 traps too much water for hydrates to readily form. Notably, after long periods of time a significant amount of hydrate does form, indicating that the water can exchange across the framework to partake in hydrate formation, yet the rate is slow as so much water is trapped.

Despite the slow growth rate resulting in the packed column experiments with 2.0 wt% and 2.5 wt% HKUST-1, the higher concentrations

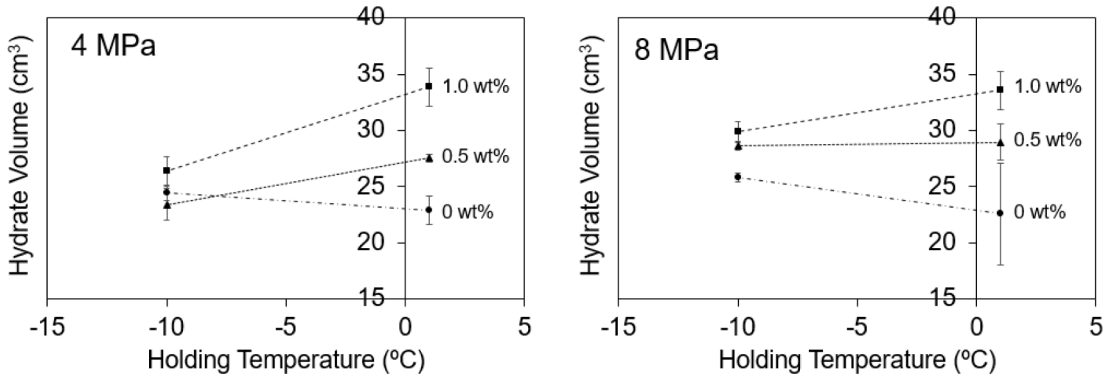

Fig. 3. The volume of hydrate formed relative to the temperature the packed column was held at for a constant pressure of (left) 4 MPa and (right) 8 MPa at different concentrations of HKUST-1.

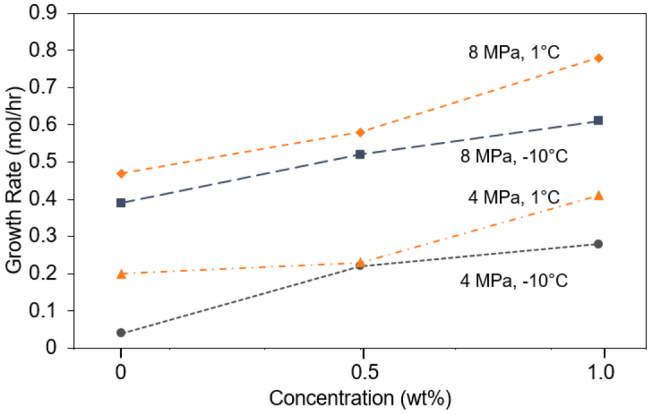

Fig. 4. Methane hydrate growth rate for the packed column without HKUST-1 and with 0.5 wt% and 1.0 wt% of HKUST-1 at four different pressure/temperature conditions. Points represent data, and dashed lines merely connect the points for convienence.

still shortened the hydrate nucleation induction time at the highest driving force conditions (8 MPa and −10 °C) by 88.4% and 93.1%, respectively, similar to the results for 0.5 wt% and 1.0 wt% (92.5% and 92.4%, respectively). This finding indicates that the chemical composition of HKUST-1 (i.e. copper nodes in the framework) affects the hydrate nucleation time significantly, most likely more than the large surface area of HKUST-1 or its methane uptake capacity.

3.3. Influence of temperature on HKUST-1 promotion performance

The conversion in the systems with HKUST-1 reaches significantly higher amounts at 1 °C versus −10 °C, an opposite trend compared to the system without HKUST-1. The difference stems from the interactions between HKUST-1 and ice. Before the system is cooled, the mild wettability of HKUST-1 keeps the water at a thin layer on the surface and in the pores, competing with methane molecules. As the system is cooled and hydrates start to form, liquid water gets trapped in the pores of HKUST-1 due to the hydrates forming at the gas/water interface. As reported in Table 1, the hydrates in the system with HKUST-1 start nucleating at ~ 0.5 °C to 1 °C. Thus, since the cooling rate is 0.55 °C/min, the system with the target holding temperature of −10 °C quickly surpasses the freezing point of ice. As ice formation competes with hydrate formation, the liquid water in the pores of HKUST-1 freezes to ice. This trapped ice does not convert to hydrates, as the diameter of the pores of the HKUST-1 are 5.9 nm and 7.0 nm, measured by a nitrogen isotherm at 77 K shown in Fig. S5, which are too small for the 1.2 nm unit cell of structure I methane hydrates.[6] In the previous work from our group on HP-DSC tests on HKUST-1, as a methane hydrate promoter, it was found that the pores of HKUST-1 experienced expansion due to ice forming inside of the pores, as evident from both a shift in the XRD pattern and a change in porosity.[40] The commercial HKUST-1 in this work was also subjected to the HP-DSC, and the XRD pattern when compared to the synthesized HKUST-1 in our previous work experienced the same shift, as shown in Fig. S5, further suggesting that ice formation takes place in the pores. Additionally, no shift in the hydrate dissociation temperature took place, indicating that the confined water did not form hydrates.[57,58] At the higher temperature of 1 °C, combined with the high pressure methane, the initial liquid water in the pores can be rapidly moved across the framework, as indicated in the literature.[49] Thus, if the temperature is kept well above the freezing point of water, than the trapped water can migrate out of the pores to form hydrates.

Interestingly, in the system with the optimal HKUST-1 concentration of 1.0 wt%, the most hydrates formed at the mildest temperature and pressure conditions tested. Formation at mild conditions is desirable as it is less energy intensive, thus making HKUST-1 an even more attractive hydrate growth promoter and potentially suitable for commercialization.

3.4. Reproducibility & recyclability

Reproducible results and recyclability of HKUST-1 impacts its efficiency and life cycle as a hydrate growth promoter. For the packed column experiments with HKUST-1, the standard deviations for the amount of hydrates formed and the nucleation induction times were relatively small, evident by standard deviations in Fig. 3 and Table 1, respectively, and did not show any trends indicating a decrease in promotion performance. This reproducibility agrees with the HP-DSC experiments on the HKUST-1 used in this study, as multiple cycles of hydrate formation and dissociation showed reproducible results with no declining promoter performance trend. As for recyclability, the overall crystallinity of HKUST-1 remained constant after multiple cycles of hydrate formation and dissociation, as evident in the XRD patterns in Fig. S5. Some studies in literature found that repeated exposure to water can degrade the structure of HKUST-1,[59] yet ethanol treatments can reverse the decomposition of HKUST-1.[60,61] In this study, the lack of any decline in performance, even after leaving wetted HKUST-1 in the packed column for more than 4 weeks, indicates that with the HKUST-1 used here, the structure can maintain chemical stability for an extensive length of time. Therefore, if any degradation of HKUST-1 is noticed overtime, then with occasional ethanol treatments to reverse the decomposition the HKUST-1 would have a long lifecycle as a methane hydrate growth promoter.

4. Conclusions

In summary, the results obtained in our previous study on the ability

of HKUST-1 promoting hydrate growth on a microscale HP-DSC (0.5 cm^3) exhibited excellent scalability to a large-scale packed column (~60 cm^3). HKUST-1 decreased the hydrate nucleation induction time in the column on average by 86.8 ± 4.1% and 86.2 ± 5.4% at a concentration of 0.5 wt% and 1.0 wt%, respectively, due to its high thermal conductivity stemming from its copper nodes and its high methane uptake providing a source of methane for hydrate formation. The thermal conductivity of HKUST-1 also led to a faster hydrate growth rate, and the magnitude of the rate increased with increasing HKUST-1 concentration. HKUST-1 also increased the quantity of hydrates formed in the column, with the highest conversion taking place at mild temperature of 1 °C with 1.0 wt% HKUST-1. Lastly, HKUST-1 exhibited reproducible results and maintained its overall structural integrity, suggesting HKUST-1 has enhanced recyclability. Therefore, combination of HKUST-1 in low concentration dispersed Chenille fabric packing in a static column shows great potential for the commercial viability of this method for the scalability of methane storage. In principle, this scalability process can be potentially extended for the effective storage of other industrially relevant gases.

Declaration of Competing Interest

The authors declare that they have no known competing financial interests or personal relationships that could have appeared to influence the work reported in this paper.

Funding

This work was supported by the National Science Foundation [CBET award # 1835924].

Appendix A. Supplementary data

Supplementary data to this article can be found online at https://doi.org/10.1016/j.fuel.2022.124920.

References

[1] Energy Information Administration U. International Energy Outlook 2019. 2019.
[2] Tanaka K, Cavalett O, Collins WJ, Cherubini F. Asserting the climate benefits of the coal-to-gas shift across temporal and spatial scales. Nat Clim Chang 2019;9:389–96. https://doi.org/10.1038/s41558-019-0457-1.
[3] Bhattacharjee G, Goh MN, Arumuganainar SEK, Zhang Ye, Linga P. Ultra-rapid uptake and the highly stable storage of methane as combustible ice. Energy Environ Sci 2020;13(12):4946–61.
[4] Yeon S-H, Seol J, Koh D-Y, Seo Y-j, Park K-P, Huh D-G, et al. Abnormal methane occupancy of natural gas hydrates in deep sea floor sediments. Energy Environ Sci 2011;4(2):421–4.
[5] Veluswamy HP, Kumar A, Seo Y, Lee JD, Linga P. A review of solidified natural gas (SNG) technology for gas storage via clathrate hydrates. Appl Energy 2018;216:262–85. https://doi.org/10.1016/j.apenergy.2018.02.059.
[6] Sloan ED, Koh CA. Clathrate Hydrates of Natural Gases. CRC Press; 2007.
[7] Hao W, Wang J, Fan S, Hao W. Evaluation and analysis method for natural gas hydrate storage and transportation processes. Evaluation and analysis method for natural gas hydrate storage and transportation processes 2008;49(10):2546–53.
[8] Cheng Z, Wang S, Xu N, Liu W, Zhao Y, Zhao J, et al. Quantitative analysis of methane hydrate formation in size-varied porous media for gas storage and transportation application. Fuel 2021;301:121021.
[9] Kumar A, Daraboina N, Kumar R, Linga P. Experimental Investigation to Elucidate Why Tetrahydrofuran Rapidly Promotes Methane Hydrate Formation Kinetics: Applicable to Energy Storage. J Phys Chem C 2016;120:29062–8. https://doi.org/10.1021/acs.jpcc.6b11995.
[10] Inkong K, Rangsunvigit P, Kulprathipanja S, Linga P. Effects of temperature and pressure on the methane hydrate formation with the presence of tetrahydrofuran (THF) as a promoter in an unstirred tank reactor. Fuel 2019;255:115705. https://doi.org/10.1016/j.fuel.2019.115705.
[11] Choudhary N, Hande VR, Roy S, Chakrabarty S, Kumar R. Effect of Sodium Dodecyl Sulfate Surfactant on Methane Hydrate Formation: A Molecular Dynamics Study. J Phys Chem B 2018;122:6536–42. https://doi.org/10.1021/acs.jpcb.8b02285.
[12] Veluswamy HP, Kumar A, Kumar R, Linga P. An innovative approach to enhance methane hydrate formation kinetics with leucine for energy storage application. Appl Energy 2017;188:190–9. https://doi.org/10.1016/j.apenergy.2016.12.002.
[13] Zeng Y, Niu X, Lei D, Liu Z, Zhu Z, Wang W. Boric acid: The first effective inorganic promoter for methane hydrate formation under static conditions. Sustain Energy Fuels 2020;4:4478–81. https://doi.org/10.1039/d0se00640h.
[14] Zhong DL, Li Z, Lu YY, Le WJ, Yan J, Qing SL. Investigation of CO2 Capture from a CO2 + CH4 Gas Mixture by Gas Hydrate Formation in the Fixed Bed of a Molecular Sieve. Ind Eng Chem Res 2016;55:7973–80. https://doi.org/10.1021/acs.iecr.5b03989.
[15] Xin Y, Zhang J, He Y, Wang C. Modelling and experimental study of hydrate formation kinetics of natural gas-water-surfactant system in a multi-tube bubble column reactor. Can J Chem Eng 2019;97:2765–76. https://doi.org/10.1002/CJCE.23515.
[16] Linga P, Daraboina N, Ripmeester JA, Englezos P. Enhanced rate of gas hydrate formation in a fixed bed column filled with sand compared to a stirred vessel. Chem Eng Sci 2012;68:617–23. https://doi.org/10.1016/j.ces.2011.10.030.
[17] Park T, Lee JY, Kwon TH. Effect of Pore Size Distribution on Dissociation Temperature Depression and Phase Boundary Shift of Gas Hydrate in Various Fine-Grained Sediments. Energy Fuels 2018;32:5321–30. https://doi.org/10.1021/acs.energyfuels.8b00074.
[18] Liu H, Zhan S, Guo P, Fan S, Zhang S. Understanding the characteristic of methane hydrate equilibrium in materials and its potential application. Chem Eng J 2018;349:775–81. https://doi.org/10.1016/j.cej.2018.05.150.
[19] Andres-Garcia E, Dikhtiarenko A, Fauth F, Silvestre-Albero J, Ramos-Fernández EV, Gascon J, et al. Methane hydrates: Nucleation in microporous materials. Chem Eng J 2019;360:569–76.
[20] Kim N-J, Park S-S, Shin S-W, Hyun J-H, Chun W. An experimental investigation into the effects of zeolites on the formation of methane hydrates. Int J Energy Res 2015;39:26–32. https://doi.org/10.1002/er.3201.
[21] García Blanco AA, Vallone AF, Korili SA, Gil A, Sapag K. A comparative study of several microporous materials to store methane by adsorption. Microporous Mesoporous Mater 2016;224:323–31. https://doi.org/10.1016/j.micromeso.2016.01.002.
[22] Zang X, Du J, Liang D, Fan S, Tang C. Influence of A-type Zeolite on Methane Hydrate Formation. Chinese J Chem Eng 2009;17:854–9. https://doi.org/10.1016/S1004-9541(08)60287-6.
[23] Zhao Y, Zhao J, Liang W, Gao Q, Yang D. Semi-clathrate hydrate process of methane in porous media-microporous materials of 5A-type zeolites. Fuel 2018;220:185–91. https://doi.org/10.1016/j.fuel.2018.01.067.
[24] Cuadrado-Collados C, Majid AAA, Martínez-Escandell M, Daemen LL, Missyul A, Koh C, et al. Freezing/melting of water in the confined nanospace of carbon materials: Effect of an external stimulus. Carbon N Y 2020;158:346–55.
[25] Cuadrado-Collados C, Fauth F, Such-Basañez I, Martínez-Escandell M, Silvestre-Albero J. Methane hydrate formation in the confined nanospace of activated carbons in seawater environment. Microporous Mesoporous Mater 2018;255:220–5. https://doi.org/10.1016/j.micromeso.2017.07.047.
[26] Mohebbi V, Naderifar A, Behbahani RM, Moshfeghian M. Investigation of kinetics of methane hydrate formation during isobaric and isochoric processes in an agitated reactor. Chem Eng Sci 2012;76:58–65. https://doi.org/10.1016/j.ces.2012.04.016.
[27] Zhang G, Shi X, Wang F. Methane hydrate production using a novel spiral-agitated reactor: Promotion of hydrate formation kinetics. AIChE J 2022;68:e17423.
[28] Taylor CJ, Miller KT, Koh CA, Sloan ED. Macroscopic investigation of hydrate film growth at the hydrocarbon/water interface. Chem Eng Sci 2007;62(23):6524–33.
[29] Cuadrado-Collados C, Farrando-Pérez J, Martínez-Escandell M, Missyul A, Silvestre-Albero J. Effect of additives in the nucleation and growth of methane hydrates confined in a high-surface area activated carbon material. Chem Eng J 2020;388:124224. https://doi.org/10.1016/j.cej.2020.124224.
[30] Casco ME, Zhang En, Grätz S, Krause S, Bon V, Wallacher D, et al. Experimental Evidence of Confined Methane Hydrate in Hydrophilic and Hydrophobic Model Carbons. J Phys Chem C 2019;123(39):24071–9.
[31] Casco ME, Rey F, Jordá JL, Rudić S, Fauth F, Martínez-Escandell M, et al. Paving the way for methane hydrate formation on metal-organic frameworks (MOFs). Chem Sci 2016;7(6):3658–66.
[32] Mu L, Liu B, Liu H, Yang Y, Sun C, Chen G. A novel method to improve the gas storage capacity of ZIF-8. J Mater Chem 2012;22:12246–52. https://doi.org/10.1039/c2jm31541f.
[33] Dongliang L, Hao P, Deqing L. Thermal conductivity enhancement of clathrate hydrate with nanoparticles. Int J Heat Mass Transf 2017;104:566–73. https://doi.org/10.1016/j.ijheatmasstransfer.2016.08.081.
[34] Pahlavanzadeh H, Rezaei S, Khanlarkhani M, Manteghian M, Mohammadi AH. Kinetic study of methane hydrate formation in the presence of copper nanoparticles and CTAB. J Nat Gas Sci Eng 2016;34:803–10. https://doi.org/10.1016/j.jngse.2016.07.001.
[35] Inkong K, Veluswamy HP, Rangsunvigit P, Kulprathipanja S, Linga P. Innovative Approach to Enhance the Methane Hydrate Formation at Near-Ambient Temperature and Moderate Pressure for Gas Storage Applications. Ind Eng Chem Res 2019;58:22178–92. https://doi.org/10.1021/acs.iecr.9b04498.
[36] Denning S, Majid AAA, Lucero JM, Crawford JM, Carreon MA, Koh CA. Methane Hydrate Growth Promoted by Microporous Zeolitic Imidazolate Frameworks ZIF-8 and ZIF-67 for Enhanced Methane Storage. ACS Sustain Chem Eng 2021;9:9001–10. https://doi.org/10.1021/ACSSUSCHEMENG.1C01488.
[37] Cuadrado-Collados C, Mouchaham G, Daemen L, Cheng Y, Ramirez-Cuesta A, Aggarwal H, et al. Quest for an Optimal Methane Hydrate Formation in the Pores of Hydrolytically Stable Metal-Organic Frameworks. J Am Chem Soc 2020;142(31):13391–7.

[38] Kim D, Ahn YH, Lee H. Phase Equilibria of CO2 and CH4 Hydrates in Intergranular Meso/Macro Pores of MIL-53 Metal Organic Framework. J Chem Eng Data 2015; 60:2178–85. https://doi.org/10.1021/acs.jced.5b00322.
[39] He Z, Zhang K, Jiang J. Formation of CH4 Hydrate in a Mesoporous Metal-Organic Framework MIL-101: Mechanistic Insights from Microsecond Molecular Dynamics Simulations. J Phys Chem Lett 2019;10(22):7002–8.
[40] Denning S, Majid AA, Lucero JM, Crawford JM, Carreon MA, Koh CA. Metal-Organic Framework HKUST-1 Promotes Methane Hydrate Formation for Improved Gas Storage Capacity. ACS Appl Mater Interfaces 2020;12:53510–8. https://doi.org/10.1021/acsami.0c15675.
[41] Chae HK, Siberio-Pérez DY, Kim J, Go YongBok, Eddaoudi M, Matzger AJ, et al. A route to high surface area, porosity and inclusion of large molecules in crystals. Nature 2004;427(6974):523–7.
[42] He Y, Chen F, Li B, Qian G, Zhou W, Chen B. Porous metal–organic frameworks for fuel storage. Coord Chem Rev 2018;373:167–98. https://doi.org/10.1016/J.CCR.2017.10.002.
[43] He Y, Zhou W, Qian G, Chen B. Methane storage in metal-organic frameworks. Chem Soc Rev 2014;43:5657–78. https://doi.org/10.1039/c4cs00032c.
[44] Li XY, Zhong DL, Englezos P, Lu YY, Yan J, Qing SL. Insights into the self-preservation effect of methane hydrate at atmospheric pressure using high pressure DSC. J Nat Gas Sci Eng 2021;86:103738. https://doi.org/10.1016/J.JNGSE.2020.103738.
[45] Sum AK, Koh CA, Sloan ED. Clathrate hydrates: From laboratory science to engineering practice. Ind Eng Chem Res 2009;48:7457–65. https://doi.org/10.1021/ie900679m.
[46] Susilo R, Ripmeester JA, Englezos P. Methane Conversion Rate into Structure H Hydrate Crystas from Ice. AIChE J 2007;53:2451–60.
[47] Wells JD, Majid AAA, Creek JL, Sloan ED, Borglin SE, Kneafsey TJ, et al. Water content of carbon dioxide at hydrate forming conditions. Fuel 2020;279:118430.
[48] Babaei H, McGaughey AJH, Wilmer CE. Transient Mass and Thermal Transport during Methane Adsorption into the Metal-Organic Framework HKUST-1. ACS Appl Mater Interfaces 2018;10:2400–6. https://doi.org/10.1021/acsami.7b13605.
[49] Gul-E-Noor F, Michel D, Krautscheid H, Haase J, Bertmer M. Time dependent water uptake in Cu3(btc)2 MOF: Identification of different water adsorption states by 1H MAS NMR. Microporous Mesoporous Mater 2013;180:8–13. https://doi.org/10.1016/j.micromeso.2013.06.033.
[50] Nguyen NN, Nguyen AV. Hydrophobic Effect on Gas Hydrate Formation in the Presence of Additives. Energy Fuels 2017;31:10311–23. https://doi.org/10.1021/ACS.ENERGYFUELS.7B01467.
[51] Andrew Lin KY, Hsieh YT. Copper-based metal organic framework (MOF), HKUST-1, as an efficient adsorbent to remove p-nitrophenol from water. J Taiwan Inst Chem Eng 2015;50:223–8. https://doi.org/10.1016/j.jtice.2014.12.008.
[52] Nguyen NN, Galib M, Nguyen AV. Critical Review on Gas Hydrate Formation at Solid Surfaces and in Confined Spaces – Why and How Does Interfacial Regime Matter? Energy Fuels 2020;34:6751–60. https://doi.org/10.1021/acs.energyfuels.0c01291.
[53] Guo Y, Xiao W, Pu W, Hu J, Zhao J, Zhang L. CH4 Nanobubbles on the Hydrophobic Solid-Water Interface Serving as the Nucleation Sites of Methane Hydrate. Langmuir 2018;34:10181–6. https://doi.org/10.1021/acs.langmuir.8b01900.
[54] Sun B, Kayal S, Chakraborty A. Study of HKUST (Copper benzene-1,3,5-tricarboxylate, Cu-BTC MOF)-1 metal organic frameworks for CH4 adsorption: An experimental Investigation with GCMC (grand canonical Monte-carlo) simulation. Energy 2014;76:419–27. https://doi.org/10.1016/j.energy.2014.08.033.
[55] Kim D, Lim H-K, Ro H, Kim H, Lee H. Unexpected Carbon Dioxide Inclusion in Water-Saturated Pores of Metal-Organic Frameworks with Potential for Highly Selective Capture of CO2. Chem – A Eur J 2015;21:1125–9. https://doi.org/10.1002/CHEM.201405360.
[56] Cha M, Baek S, Morris J, Lee JW. Hydrophobic Particle Effects on Hydrate Crystal Growth at the Water-Oil Interface. Chem – An Asian J 2014;9:261–7. https://doi.org/10.1002/ASIA.201300905.
[57] Chong ZR, Yang M, Khoo BC, Linga P. Size Effect of Porous Media on Methane Hydrate Formation and Dissociation in an Excess Gas Environment. Ind Eng Chem Res 2016;55:7981–91. https://doi.org/10.1021/acs.iecr.5b03908.
[58] Borchardt L, Casco ME, Silvestre-Albero J. Methane Hydrate in Confined Spaces: An Alternative Storage System. ChemPhysChem 2018;19:1298–314. https://doi.org/10.1002/cphc.201701250.
[59] Domán A, Czakkel O, Porcar L, Madarász J, Geissler E, László K. Role of water molecules in the decomposition of HKUST-1: Evidence from adsorption, thermoanalytical, X-ray and neutron scattering measurements. Appl Surf Sci 2019; 480:138–47. https://doi.org/10.1016/J.APSUSC.2019.02.177.
[60] Majano G, Martin O, Hammes M, Smeets S, Baerlocher C, Pérez-Ramírez J. Solvent-Mediated Reconstruction of the Metal-Organic Framework HKUST-1 (Cu3(BTC)2). Adv Funct Mater 2014;24:3855–65. https://doi.org/10.1002/adfm.201303678.
[61] Sun X, Li H, Li Y, Xu F, Xiao J, Xia Q, et al. A novel mechanochemical method for reconstructing the moisture-degraded HKUST-1. Chem Commun 2015;51(54): 10835–8.